# Effect of the inclusion of optical antennas in increasing the sensivity of biosensors

Rodolfo Costa Gomes Rodrigues, Mestrado em Engenharia Eletrotécnica e de Computadores

Instituto Superior Técnico, Academia Militar

e-mail: rodolfo-cost@hotmail.com

**Abstract: The progress in the development of nanotechnologies has been increasing since the beginning of the century. New devices with small dimension such as nanoantennas start to become more and more common nowadays, an there is a good reason for that. These devices allow to create simple systems with great utility at a very low cost.**

**In this article will be studied de behaviour of optical antennas which the dimensions of the apertures are smaller than the wavelength. The structure of the antenna will be made of silicon and the material of the metallic elements will be determined based on the antenna response. After that the magnetic field propagation will be studied in order to comprehend how light travel through the skin layers, and how can we analyse the blood oxygenation and the heart rate using a biosensor. Simulation's result were obtained by using COMSOL Multiphysics.**

## 1. INTRODUCTION

Since the beginning of human existence, we fascinate about the power of light. Due to technologic advances the light, is not only used to illuminate the darkness, like our ancestors did in the past, but also has a fundamental role in modern society. Nowadays, light is used from the more basic functionalities as lighten the roads and houses at night, to the appliances that change the world as the global communications systems and in the medicine.

The evolution of science has generated great discoveries and innovations in the field of nanotechnology, allowing the discovery of new products with an increasing performance. These products include optoelectronic devices, such as nano-antennas or optical antennas with increasing applications in the field of medicine, contributing to the development of the so-called nanomedicine.

Nanomedicine is a sub-area of medicine that has emerged with the aim of promoting advances in nanotechnology applications in the area of traditional medicine. Nanotechnology-based devices have several applications to aid in the diagnosis and treatment of patients through less intrusive or even non-intrusive techniques, which was not possible with previous technologies. The use of nanotechnology-based devices makes it easier to obtain data due to its practicality compared to older technologies.

Taking heart rate measurement as an example, to perform this task we need a sphygmomanometer to do this. This device is suitable for medical use as it is reliable, accurate and easy to use, however it has the disadvantage of not allowing in real time reading in a practical way to a patient, unlike a device based on nanotechnology that allows to go along with the patient and constantly monitor in real time the patient's heart rate and other relevant parameters. The advantages that nanotechnology devices bring are evident in several areas where real-time monitoring is not only useful but extremely necessary.

One of the areas where these nanotechnology devices have a high impact is in the military environment. These devices, based on nanotechnology, are very useful in this area, bearing in mind that military personnel deployed in to the battlefield are subject to both environmental and behavioural conditions, when dealing with different risk situations, very different from those they are used to in National Territory. Thus, due to the nature of a soldier's mission, the high physical intensity and the subjection to adverse environments, the monitoring of soldiers is extremely important, to preserve their health, allowing them to be assisted as soon as possible in case of need. This contributes to an optimization of the performance of the deployed forces, namely avoiding unnecessary casualties in the military forces. These devices are, however, useful both in real scenario environments, in the case of missions where the military is deployed to perform their functions, as well as in simulation environments, where the military is in training or during the performance of courses where the military's physical capabilities are exploited to the limit. In both cases, these devices have as their main objective to permanently monitor the physical condition of the military.

In the case of medicine, we have biosensors that are widely used in obtaining and transmitting biometric data and in the non-invasive detection of diseases. One of the advantages that these new technological devices bring is the construction of increasingly sensitive biosensors, making the non-invasive detection of diseases easier than ever.

## 2. STATE OF THE ART

### *A. Biometric parameters*

Biometrics [bio(life) + metrics(measurement)] is the study and measurement of physical and behavioural characteristics of living beings. This area thus has several applications, the one that interests us in particular is biometrics associated with the human being. Of the various applications associated with biometrics, the best known are criminal identification and access control, either through facial recognition or through fingerprints.

One of the most important applications of biometrics in today's world is, without a doubt, monitoring the vital parameters of human beings, which helps health professionals to better understand the health status of their patients.

Before the existence of sensors for measuring biometric parameters, these were measured in an archaic way, and often through common sense, placing the hand on the forehead to determine whether it is hot or cold as is the case with measuring body temperature or counting the number of times we feel the blood flowing through the veins to measure the heart rate. Although there is no record of who invented the thermometer, there have been many attempts, throughout history, to create a device that was sensitive to temperature, since 3 BC. in which Philon of Byzantium created a device sensitive to thermal variation, passing by Galileo Galilei who, in 1592, built a thermoscope, not forgetting the physicist Daniel Fahrenheit who developed the mercury thermometer, widely used in recent centuries, until the introduction of recent ones such as thermocouple and infrared thermometer. As for measuring heart rate, there are also reports that ancient civilizations were already trying to understand how the heart worked, but the most significant discoveries began after Willem Einthoven, the father of electrocardiography, created the first device that reliably measured the heart rate frequency. The sphygmomanometer was later developed by Samuel Von Basch, which today is a device widely used by doctors and nurses in hospitals, clinics and health centers worldwide.[1]

These are examples of just 2 biometric parameters that can be measured using specific devices developed for that particular function, but there are others that are also important for our daily lives.

Within the biometric parameters we must mention a special group consisting of the so-called vital parameters:

- Heart rate
- Respiratory frequency
- Blood pressure
- Body temperature

These parameters are indicators of vital functions and allow the assessment of a patient's physical condition.

### *B. Biometric parameters*

Blood is responsible for transporting oxygen to different parts of our body, ensuring a vital flow for human beings. When the amount of oxygen reaching the cells is insufficient, serious problems can occur, putting a person's life at risk. Therefore, it is essential to monitor the heart rate and oxygen saturation in the blood, whether for people who suffer from respiratory problems, or for people who practice high-intensity activities.[2][3]

The first methods used to measure oxygen saturation in the blood were based on invasive collection techniques, that is, in these cases it is necessary to take a blood sample from the person in question and then analyse the sample in the laboratory, it is not a case in which it is possible to have a real-time reading, as well as not being, at all, a convenient and practical method

Oximetry is the technique that makes it possible to measure the oxygen saturation in the blood using optical methods. Although the blood is inside the human body, it is possible to determine its oxygen saturation through optical means.

Non-invasive methods are the most used and marketed either in a professional environment, such as hospitals and high-performance centers, or in leisure when practicing physical exercise. The advantage of non-invasive methods is that they provide users with continuous and practical monitoring.[4]

Non-invasive methods are essentially limited to spectrophotometric methods. These make use of the optical properties of materials, such as absorption and reflection, to determine the constituents of a given sample.

Places where an oximeter is most common are on the wrists, fingers, earlobes, or chest. These zones are preferable because the blood vessels are located close to the surface of the skin, or because the inflow of blood to these zones is greater, thus making it possible to obtain more accurate readings of blood oxygen saturation and heart rate[5]

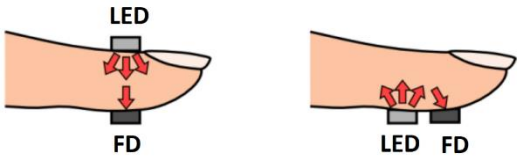


*Figure 1 - Oximeter's operation types, by transmission (on the left), and by reflection (on the right)*[6]

### *C. Photoplethysmography*

Photoplethysmography is an optical method that collects information about changes in blood volume in a certain region of the human body, this signal is commonly collected through an oximeter. The graph that results from recording this signal as a function of time is called a photoplethysmogram (PPG), and represents the variation in light absorption in tissues and blood. with the signal received on the photodiode. As the diameter of blood vessels increase during systole, the attenuation of radiation will also be greater in the case of transmission. In the case of reflection, the surface area of the blood vessel is greater, so the intensity of the reflected radiation will also be greater.[7][8]

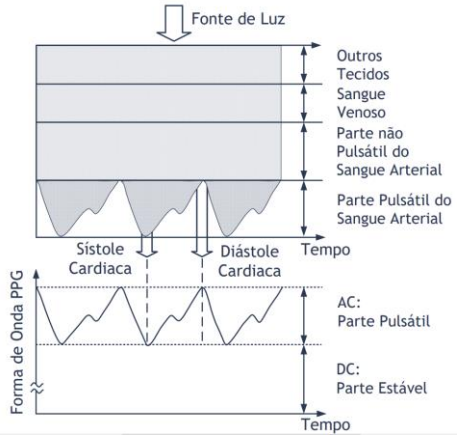


*Figure 2 – Signal components that make up the heart pulse*[9]

To develop a device to measure heart rate, it is first necessary to determine the most appropriate place to place this sensor, as it uses phenomena such as reflection or absorption of blood to determine heart rate.

As previously mentioned, the alternatives to consider for the placement of the sensor are as follows:

- Place the sensor on the finger (ring type device)
- Put the sensor on your wrist (bracelet-type device)
- Place the sensor on the chest (band-type device, often used by high competition athletes)

### *D. Nanoantennas*

Antennas are a very important element nowadays; they are responsible for establishing wireless communications that are

present in all our daily lives. Antennas are responsible for converting the electric field into a wave that propagates in space. Nanotechnology is the science that studies the behaviour of materials at the nanometer scale, involving structures with dimensions of the order of the nanometer (nm or ×10-9 m). With the evolution of technology, this science was diversified into the vastest areas, bringing benefits to all of them. Nanoantennas appeared in the last century and since then, better and more efficient antennas have been developed.

The theory of how nanoantennas work follows the same laws as traditional radiofrequency (RF) antennas, the range of the spectrum where these antennas operate is different. The radiation falls on the antenna surface, introducing an oscillation in the electrons present in the antenna with the same frequency as the received light, this oscillation is caused by the electric field of the incident radiation. A receiving nanoantenna is nothing more than a converter of incident light (radiation of frequency corresponding to the optical band) in a strong confined field, in the same way that an emitting nanoantenna is a converter of a strong confined field into radiation of a corresponding frequency to the optical band.[10]

The antennas can be classified into 4 groups according to their type:

- Electrically small antennas (very small dimensions compared to wavelength λ)
- Resonant antennas (monopoles, dipoles, Yagi-Uda, etc)
- Broadband antennas (used in terrestrial television broadcasting)
- Opening antennas (horn antennas)

Optical antennas, despite respecting the same laws as RF antennas, are not RF antennas reduced to a nanometric scale. Basically, when we dimension an antenna, we aim to optimize the communication between the emitter and the receiver in order to reduce energy consumption.

Optical slit antennas are a type of antenna of relatively simple complexity, these have the advantage of having physical phenomena when subjected to interactions with electromagnetic radiation. Bethe developed the theory that as the slit diameter decreases relative to the wavelength of the radiation, the transmitted power will also decrease. This theory was incorrect, and only later was discovered the phenomenon called EOT. This discovery has enabled major developments during the last decades.

### *E. Extraordinary Optical Transmission*

Extraordinary optical transmission (EOT) is a phenomenon in which increased transmission of radiation is observed when it passes through slits, smaller than the wavelength, between metallic elements, which are repeated periodically. The material of which is made must consist of conducting elements. Through EOT it is possible to increase the transmission efficiency by several orders of magnitude, larger than would be expected through classical theory. This phenomenon was discovered in 1998 and is explained through the resonance of surface plasmons (PPS), not only in regions of the visible but also outside the optical regime on very few occasions, as recent studies show.

The discovery of the EOT allowed the development of the area of components based on photonics, for example the photonic integrated circuits, which are similar to electronic integrated circuits, but operate through photons, a whole new range of possibilities was opened with the study of the phenomena explained by the EOT

### *F. Antennas Sensibility*

Sensitivity measures the degree to which the output changes when variations in the input are produced, written another way, it is the minimum value of the input parameter required to produce a change at the output. For example, temperature is a parameter that is measured by the thermometer, which in the case of atmospheric temperature varies throughout the day. This way of defining a sensor leads to some limitations being established, such as the accuracy of the measurement. Although a thermometer shows the temperature of the air, this value may not be exactly correct, either due to a defect in the calibration of the thermometer or due to limitations on the number of digits that can be displayed. By increasing the transmission efficiency, derived from the presence of the EOT phenomenon, it is possible to increase the sensitivity of a sensor. This method of increasing the sensitivity of sensors is quite advantageous, since it can be done at a very affordable cost and without increasing the power consumption of the sensor.[11]

### *G. Superficial Plasmons*

The existence of surface plasmons results from the interaction between the metallic structures and the incident light, and this phenomenon is observable, practically only in the visible spectrum, since outside these regions there is no resonance of surface plasmons.

Surface plasmons were discovered in 1950 by Ritchie, and are defined as waves propagating in the metallic nanostructures of a given conductor. Surface plasmons concentrate light into the structure's crevices, significantly increasing the electric field, which can increase by several orders of magnitude. Through these it is possible to control the interactions between light and matter and increase light transmission using periodically spaced slits.

When light strikes the zone that separates the dielectric from the metal, it generates surface oscillations that propagate collectively along the structure, these oscillations are directly related to the SPP. To be observed SPP requires that the metal elements have a dielectric constant with the real part negative for the wavelength of the incident radiation.

Surface plasmon based antennas can be divided into two different types, SPR surface plasmon resonance or LSPR localized surface plasmon resonance.

### *H. SPR proprieties*

SPRs are charge oscillations of the PPS present at an interface composed of two media, for example a metal and a dielectric. The charge density is associated with the electromagnetic wave, the field vector reaches its maximum at the location where it interacts with the interface and decays with distance and between the media. Although SPR biosensors work with a very high sensitivity, they are not suitable for biomolecules present in low concentrations as is the case in the blood present in humans.

### *I. LSPR proprieties*

LSPR-based biosensors rely on the phenomenon of surface plasmons located at the resonance frequency, the particle extinction reaches a maximum that is dependent on the refractive index of the medium and the size and shape of the metallic element.

If variations in the refractive index of the medium are induced, it can be seen that the maximum power will vary as well as the wavelength for which the maximum LSPR peak

exists.

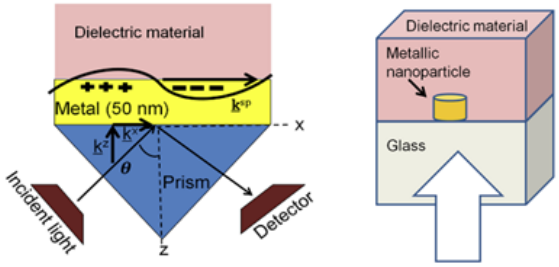


*Figure 3- principle of SPR(left) and LSPR(right)*

## 3. OXIMETRI FUNDAMENTALS

### A. *Theoretical Fundaments*

The lungs are responsible for gas exchange, expelling carbon dioxide and capturing oxygen, which is then transported to all parts of the body through the blood. The protein present in the blood that is responsible for transporting the blood is hemoglobin. Hemoglobin can be associated with various elements, when it is associated with oxygen it is called oxyhemoglobin (HbO2), when it loses its bond with oxygen atoms it is called deoxyhemoglobin (Hb). These are the main forms of hemoglobin that can be found in the blood. When a person inhales fumes such as carbon monoxide, the hemoglobin will bond with carbon monoxide, forming carboxyhemoglobin, and making oxygen transport impossible, as will inhaling nitrates, nitrites, and chlorates, which form methemoglobin.[12]

The absorption of light by hemoglobin varies with the oxygen saturation present in the blood. Oxyhemoglobin makes the blood lighter in color and deoxyhemoglobin makes it darker. This phenomenon of blood color variation is due to the fact that the two types of hemoglobin have different optical spectra. Figure 10 represents the absorption spectrum of hemoglobin as a function of the wavelength of radiation in the infrared and visible regions.

Analysing Figure 4 we can see that the greatest differences occur in the 650 nm zone, where the absorption by deoxyhemoglobin is much more significant than oxyhemoglobin and in 1000nm we observe the opposite, oxyhemoglobin has a higher absorption than deoxyhemoglobin[12][13]

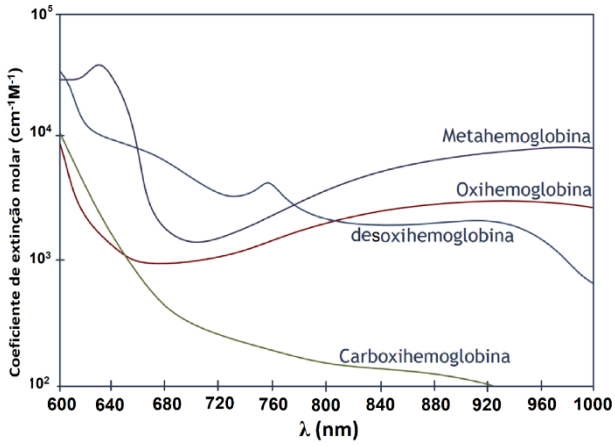


*Figure 4 . Molar extinction coefficient of hemoglobin components*[14]

For the wavelengths in the 650nm and 1000nm zone, the existence of different absorptions for different wavelengths allows the measurement of blood oxygen saturation and other relevant parameters provided by the oximeter. Oxygen saturation is calculated from the following equation, which relates the amount of oxyhemoglobin to the total amount of hemoglobin, obtaining the relative amount of oxyhemoglobin.

$$SO_2 = \frac{c_{HbO_2}}{c_{Hemoglobina}} \quad [1]$$

For an oximeter with only two different wavelengths of operation, it is not possible to determine the amount of hemoglobin harmful to health, namely methemoglobin and carboxyhemoglobin, so the total hemoglobin will be given only by the amount of oxyhemoglobin plus the amount of deoxyhemoglobin.

$$c_{Hemoglobina} = c_{HbO_2} + c_{Hb} \quad [2]$$

Putting the equations 1 and 2 together we get the following equation.

$$SO_2 = \frac{c_{HbO_2}}{c_{HbO_2} + c_{Hb}} \quad [3]$$

If the intention is to develop a more advanced monitoring system that also allows for the analysis of hemoglobin types other than those fundamental to the functioning of the human body, it would be necessary to analyse the absorbance as a function of wavelength by also taking into account the absorption spectrum of the hemoglobin variants.[15]

### B. *Lamber-Beer Model*

According to the Lambert Beer model, light is attenuated when it propagates through a medium, part of the radiation is transmitted and part is absorbed. For the transmitted part of the radiation the model states that the decay is exponential as a function of the distance travelled according to the following equations.[14][16], [17]

$$I_t = I_0 e^{-\alpha} \quad [4]$$

$$\alpha = \varepsilon dc \quad [5]$$

$I_t$ is the light transmitted to the medium, α is the absorption of the medium, ε is the extinction coefficient, d is the distance travelled in the medium, and c is the concentration of the medium. As a function of α the equation can be written as follows.

$$\alpha = -log_{10}(\frac{I_t}{I_0}) \quad [6]$$

The constitution of blood is mostly formed by oxyhemoglobin and deoxyhemoglobin, so it is possible to write the following equation, considering that the total absorption will be the sum of the absorptions of each of the constituents of blood for a given wavelength.

$$\alpha_{sangue} = \varepsilon_{HbO_2} d_{HbO_2} c_{HbO_2} + \varepsilon_{Hb} d_{Hb} c_{Hb} \quad [7]$$

$\varepsilon_{HbO_2}$ represents the extinction coefficient of oxyhemoglobin, this value is dependent on the wavelength of the incident radiation, $\varepsilon_{Hb}$ is the extinction coefficient of deoxyhemoglobin, this value is also dependent on the wavelength of the incident radiation, $d_{Hb}$ and $d_{HbO_2}$ are the

distances covered in oxyhemoglobin and dioxyhemoglobin respectively. $c_{HbO_2}$ is the concentration of oxyhemoglobin in the blood and $c_{Hb}$ is the concentration of deoxyhemoglobin in the blood.

The radiation absorbed by bone tissue, muscle tissue, and the skin layer is always constant and independent of the cardiac cycle. In the case of blood vessels, the absorption will vary, during the cardiac cycle. The transmitted radiation, both during systole and diastole can be calculated using the following equation.

$$\frac{I_{\,sístole}}{diástole} = \\ = I_0 e^{-\alpha_{fixa}} e^{-[\,\varepsilon_{HbO_2} c_{HbO_2} + \varepsilon_{Hb} c_{Hb}]\, d_{percorrida}} \quad [8]$$

$\alpha_{fixa}$ is the absorption of the tissues mentioned in the previous paragraph.

The $d_{percorrida}$ varies depending on the cardiac cycle, i.e., the electromagnetic radiation will travel different distances depending on whether it is during systole or diastole, causing the total attenuation of the path to suffer small variations, and it is through these small variations that it is possible, using optical means, to observe the variation of blood flow and in turn determine the heart rate. To determine the blood oxygenation, we need at least 2 radiations with different wavelengths as mentioned above. Using the previous equation, we can specify it for the two different situations.

$$I_{diástole} = I_0 e^{-\alpha_{fixa}} e^{-[\,\varepsilon_{HbO_2} c_{HbO_2} + \varepsilon_{Hb} c_{Hb}]\, d_{diástole}} \quad [9]$$

$$I_{sístole} = I_0 e^{-\alpha_{fixa}} e^{-[\,\varepsilon_{HbO_2} c_{HbO_2} + \varepsilon_{Hb} c_{Hb}]\, d_{sístole}} \quad [10]$$

Putting the intensity of diastole as a function of systole we get the following equation.

$$k = \frac{I_{diástole}}{I_{sístole}} \\ = e^{-[\,\varepsilon_{HbO_2} c_{HbO_2} + \varepsilon_{Hb} c_{Hb}]\,[d_{diástole} - d_{sístole}]} \quad [11] \\ = e^{-[\,\varepsilon_{HbO_2} c_{HbO_2} + \varepsilon_{Hb} c_{Hb}]\,\Delta d}$$

$\Delta d$ is the difference between the distances the radiation travels between the systole and diastole phases. In order to eliminate the variable Δd from the equation we can compare the existence of two different radiations with different wavelengths $\lambda_1$ and $\lambda_2$.

$$k' = \frac{\ln(k_{\lambda 1})}{\ln(k_{\lambda 2})} \\ = \frac{\ln\left[I_0 e^{-\alpha_{fixa}} e^{-[\,\varepsilon_{HbO_2(\lambda 1)} c_{HbO_2} + \varepsilon_{Hb(\lambda 1)} c_{Hb}]\,\Delta d}\right]}{ln\left[I_0 e^{-\alpha_{fixa}} e^{-[\,\varepsilon_{HbO_2(\lambda 2)} c_{HbO_2} + \varepsilon_{Hb(\lambda 2)} c_{Hb}]\,\Delta d}\right]} \quad [12] \\ = \frac{\varepsilon_{HbO_2(\lambda 1)} c_{HbO_2} + \varepsilon_{Hb(\lambda 1)} c_{Hb}}{\varepsilon_{HbO_2(\lambda 2)} c_{HbO_2} + \varepsilon_{Hb(\lambda 2)} c_{Hb}}$$

### *C. Oximetry limitations*

Oximetry presents several limitations that directly affect the reliability of the results obtained when a patient is analysed.

First of all, it is necessary to mention the inability of systems that use only two different wavelengths to analyse blood oxygenation. Since some approximations are considered, such as the fact that hemoglobin is composed only by oxyhemoglobin and deoxyhemoglobin, the system is not able to distinguish the presence of other types of hemoglobin that are dangerous to our health. In this case a patient who has been referred to the emergency room because of carbon monoxide inhalation, if a simpler system of only two frequencies is used, it will not be possible to diagnose the excessive presence of carboxyhemoglobin.[18]

In addition, it is important to mention the low reliability associated with oxygen saturation for values below 70% since the devices cannot be calibrated for values in that range. This limitation becomes a problem for new-borns since blood oxygen saturation ranges from 20% to 75%.[18]

Finally, it is important to mention the reliability of the equipment while performing movements and other activities, since they cause distortions in the signal. Although these distortions have small amplitude, they have a significant impact, requiring post-processing of the signal to correct these disturbances.

### *D. Skin Optical Properties*

Human skin behaves like a heterogeneous medium where blood is variably distributed spatially. The skin can be divided into 3 different main layers: the epidermis, the dermis, and the hypodermis.

The epidermis is the most superficial layer of the skin, which is in contact with the environment and its thickness varies slightly depending on body location, with the most common size being around 100μm. In this layer there is no blood stored or circulating.

The dermis is the intermediate layer of the skin, located between the epidermis and the hypodermis, this is formed by a connective tissue and therefore blood vessels are present in this layer. The thickness of this layer varies from 500μm to 4mm.

The hypodermis is the innermost layer of the skin and is responsible for insulating the body from external temperatures. This layer consists among other things of blood vessels and has a typical thickness that varies from 1 to 6 mm.

When light strikes the skin surface, 4 phenomena can be described that describe the optical behaviour of light on the skin:

- Reflection
- Transmission
- Absorption
- Dispersion

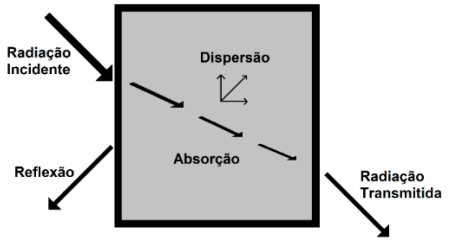


*Figure 5 - Light behaviour when passing through a medium with different refractive index*[19]

Figure 5 represents the phenomena that describe the behaviour of light when it strikes a medium with a refractive index different from the first, in this case, the medium highlighted in gray is considered a homogeneous medium, which is not the case with biological tissues.

The Reflection of light depends on the angle of incidence and the media that light passes through (air and biological tissues of human beings) and can be studied based on the laws of Fresnel Ansari and Vaughan in a more simplistic way, when biological tissues are considered as homogeneous. [19][20]

Light transmission depends on the optical properties of the biological tissues of the human body such as the refractive index, scattering and absorption of light. These properties determine how light interacts with the tissues of the human body, so we first have to study the properties of the human biological tissues in order to better understand how light behaves in this medium.

Absorption occurs in all layers of the skin and varies depending on the wavelength of the emitted radiation. To characterize the absorption of a medium, we define that the absorption coefficient (α) is the probability that a photon is absorbed in a medium when it travels a distance x. Optical absorption in biological tissues occurs primarily due to the presence of hemoglobin, melanin, and water. Hemoglobin is found in the blood circulating in blood vessels in deeper layers of the skin. Water is everywhere in our body, being the main constituent of our cells. Melanin is found in the top layer of the skin and is responsible for giving our skin its tone and protecting us from the most dangerous radiations, for this reason melanin has a significant absorption for shorter wavelengths. The absorption by hemoglobin varies depending on the oxygen saturation in the blood (SpO2), which can have a high concentration of oxygen (oxygenated hemoglobin) or a low concentration (deoxygenated hemoglobin).

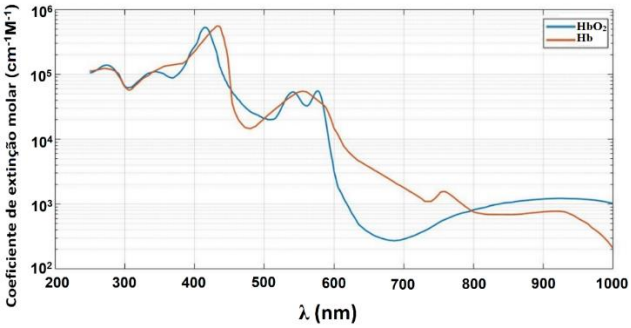


*Figure 6 - Molar extinction spectrum for oxygenated and deoxygenated hemoglobin*[20][21][22]

Figure 6 represents the molar extinction coefficient as a function of wavelength of incident radiation for oxygenated and deoxygenated hemoglobin. The molar extinction coefficient is the probability that a photon interacts with its medium when it travels a distance of length x. Absorption and scattering are considered to be an interaction between the photon and the medium in which it is propagated. Since the scattering is related to the refractive index of the medium in which the radiation is propagated and the refractive index of hemoglobin and the refractive index of the skin are practically constant along the visible band, we can disregard the effect of scattering due to the low refractive index of the skin and due to the distance that light travels in the layers of the skin.

The presence of water covers about 70% of our body, being a significant value to taken into account. Next, the graph of the absorption of water as a function of wavelength is presented in Figure 7.

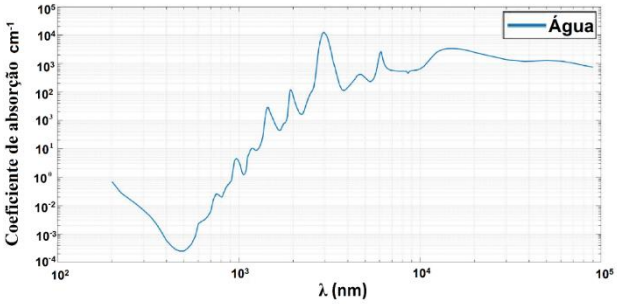


*Figure 7 - water absorption spectrum*[20][21][23]

Human beings present diverse skin tones, hair and eye colours. This diversity is due to the interaction of various pigments such as carotenoids, hemoglobin and melanin, the latter being responsible for promoting coloration. Melanin is present in the epidermis and is responsible for protecting our body from harmful UV radiation. When light falls on the skin, our body is stimulated to produce more melanin in order to absorb most of the incident radiation. Figure 8 show the two types of melanin that are eumelanin and pheomelanin.

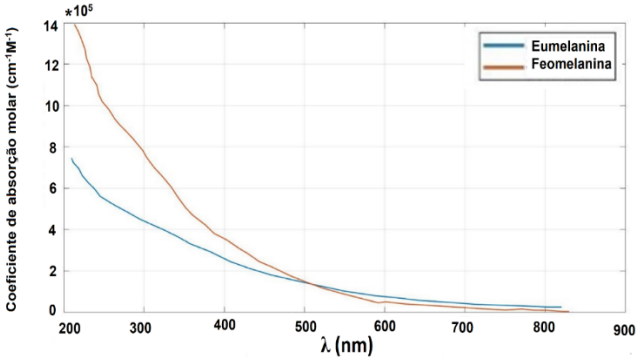


*Figure 8 - Melanin absorption spectrum (eumelanin and pheomelanin)*[24], [25]

## 4. RESULTS

### A. *Introduction*

The results are obtained through simulations performed using the COMSOL Multiphysics program, which presents the simulation results as graphs using the finite element method. All graphs presented are level curves representing the field radiated by the antenna as a function of its location. The irradiance is characterized by the modulus of the total electric field normalized to the squared incident electric field $|E/E_0|^2$. The normalization of the field allows us to immediately identify whether the phenomenon of extraordinary optical transmission occurs or not, since in the affirmative case the normalized field after the slits must have a value greater than 1

- $\lambda_0$=Lambda0 represents the wavelength of the incident radiation used in the simulation
- E0=$1 \times 10^{-6}$ [V/m] represents the amplitude of the incident electric field
- slit_size= $\lambda_0$ represents the length of the metal element sections
- Thickness=$3 \times 10^{-7}$ m represents the thickness used for the metal element sections
- spacing =$\lambda_0/2$ is the spacing between the sections of the metallic elements

*B. Cutline Study*

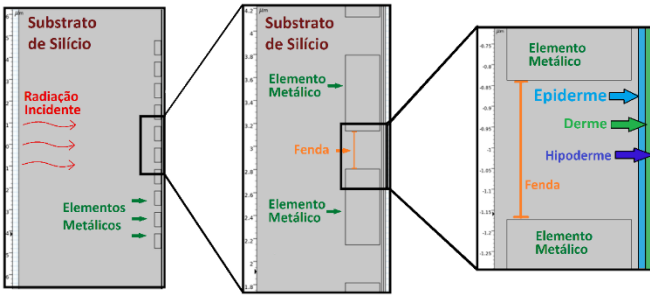


*Figure 9 - Model representation scheme used in COMSOL Multiphysics*

Figure 9 represents the schematic of the model used in COMSOL during the simulations. At first the model is only composed of the silicon substrate and the metallic elements, only later in the real model will the skin layers be added.

The antenna under study is composed of a silicon substrate where the radiation propagates in the horizontal direction and in the direction from left to right, as represented in Figure 9. The metal elements are arranged vertically near the right edge of the substrate, the spacing between the elements is called the gap and is wavelength dependent by the equation spacing=$\lambda/2$.

The objective of this first study is to determine the distance between the metallic elements and the cutline so that the intensity of the received field is maximum along the cutline, thus to be determined the maximum field the following simulations were performed.

Successive cutlines were placed with distances of $\lambda/40$, $\lambda/35$, $\lambda/30$, $\lambda/25$, $\lambda/20$ $\lambda/15$, $\lambda/10$ and $\lambda/5$, in Figure 10 are represented 4 examples of the cutlines that were studied.

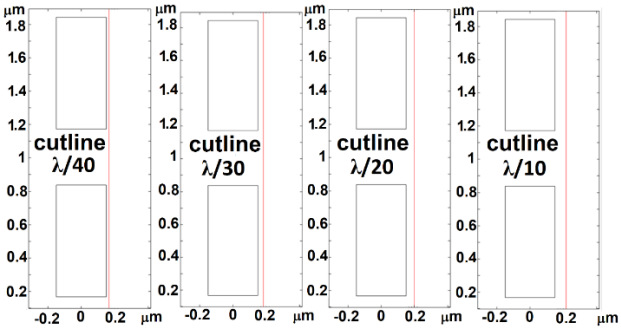


*Figure 10 - Cutlines location during simulation*

In total 8 distanced cutlines were simulated as shown in the figure above. After testing all these alternatives, we obtained the following irradiation diagrams represented in Figure 11. In this figure are also represented the vertical black lines that represent the lateral limits of the metallic elements

Figure 11 show the results obtained for the simulation, where cutline 1 corresponds to a spacing of $\lambda/40$ and cutline 8 corresponds to a spacing of $\lambda/5$. As can be seen, the best performing cutline was cutline 1, and this is the reference for all the next simulations performed.

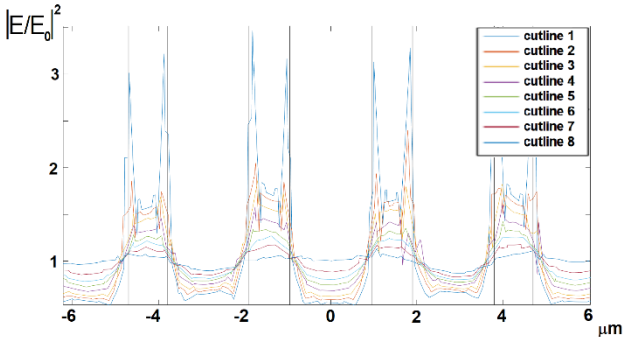


*Figure 11 - Intensity if radiation according to cutline location in detail*

After having determined the distance from the cutline for which the field was maximum, the study of the influence of a set of factors follows, with the same objective of studying which of the alternatives presents better results

The factors to be studied that influence the received field are the following

- Frequency of the incident radiation
- Material constituting the metallic elements
- Arrangement scheme of the metallic elements

The wavelengths of the radiation to be studied were as follows:

- 530nm
- 540nm
- 660nm
- 670nm
- 950nm
- 960nm

The arrangement schemes of the metal elements used were as follows:

- Rectangular
- Circulars
- Rectangular conjugated with rectangular
- Rectangular conjugated with circulars

Figure 12 shows in more detail the dimensions of the metallic elements and spacings used during the simulations. This figure was designed specifically to demonstrate in detail the schemes used, as it is not possible to obtain this same representation directly from COMSOL.

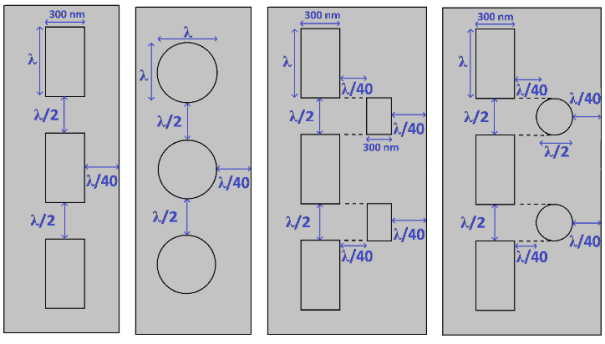


*Figure 12 - arrangement of the metallic elements used during de simulations*

By observing Figure 13 and Figure 14 and analysing Table 1 it can be seen that the best performances are registered when the metallic elements are made of platinum and when the wavelength of the incident radiation is 950nm and 960nm. The

worst performances are registered for aluminium for the wavelengths of 950nm and 960nm. With regard to the figures, it is easy to distinguish the location of the metallic elements since the graphs show fairly uniform values between them.

It is important to note that for all cases present in the table, the values of the normalized field are always greater than 1, i.e., the field intensity at the output of the antenna is always higher than the input signal, so we can say that in all cases we are amplifying the signal through the phenomenon of extraordinary optical transmission.

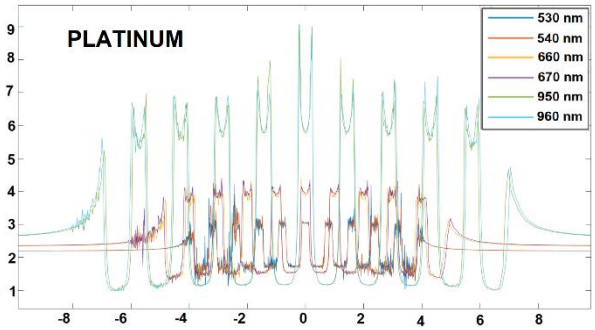


*Figure 13 - Normalized field at the antenna output when platinum rectangular metallic elements are used*

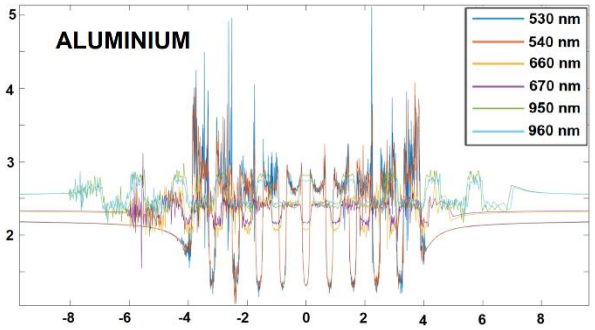


*Figure 14 - Normalized field at the antenna output when aluminium rectangular metallic elements are used*

*Table 1 - maximum value of the normalized field at the antenna output*

| Campo máximo | 530nm | 540nm | 660nm | 670nm | 950nm | 960nm |
|---|---|---|---|---|---|---|
| Platina | 4.2 | 3.9 | 4.4 | 4.4 | 9.0 | 8.9 |
| Alumínio | 5.1 | 4.0 | 3.0 | 3.1 | 3.0 | 2.8 |

Analysing all the cases studied it is possible to conclude that for all cases the effect of extraordinary optical transmission is present, since the normalized field at the antenna output is always greater than 1. The main objective is to maximize the field at the output of the antenna, and through the data presented it is possible to determine that the best option occurs in the situation where we use rectangular platinum metallic elements, for a wavelength of 950nm, so all future simulations will make use of these specifications.

### *C. Results Optimization*

COMSOL Multiphysics uses the finite element method to calculate the electric field values along the model, using meshes to solve the systems of equations that describe the problem. Initially, for the determination of the cutlines and for the analysis of the radiation wavelength, the arrangement schemes and the material constituting the metallic elements, only triangular meshes predefined by the program were used. This mesh demonstrated a good performance when it came to model processing and also presented a good quality of results.

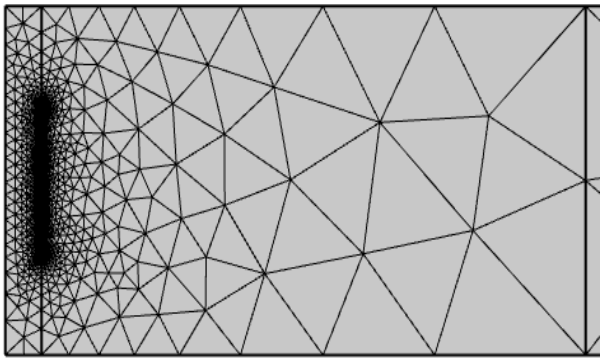

*Figure 15 - initially used mesh, generated automatically by COMSOL*

To perform the simulations with the several layers of skin integrated in the model the mesh defined by COMSOL was no longer advantageous, since for distances too far from the emission source the data obtained was quite scarce not allowing to analyse the model in the best way. In Figure 16 it can be seen that the density of points where the field is analysed is too low, making it impossible to obtain reliable results for the model.

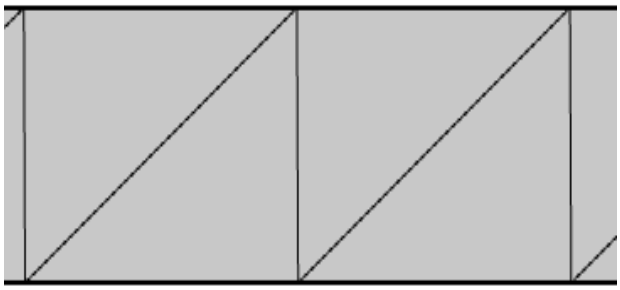

*Figure 16 - Mesh generated automatically by COMSOL, at a point away from the emission source*

In order to solve the mesh density problem, a user-controlled alternative was generated, the mesh used was of the triangular type, in the geometry scale parameters it was set that x-direction scale= 40 and y-direction scale=40. In entity control the number of iterations was set to 4 and the Maximum element depth to process was set to 4.

In Figure 17is represented the manually defined mesh, as it is possible to verify both on the left and right boundary we obtained a good density of points, obtaining a good balance between the mesh performance and the data processing time.

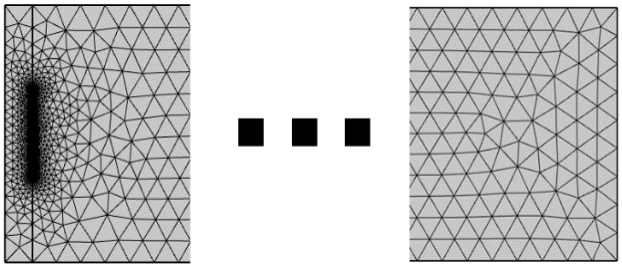

*Figure 17 - Manually defined mesh in COMSOL*

In Figure 18 it is possible to observe the differences in performance between the two meshes, in the first case where we use the automatically generated mesh, the reduced density of analysis points leads the graph to present the electric field behaviour in a wrong way, the fact that there are a low number of analysis points leads to approximations that induce an error compared to the real value of the field. In the second case where we use the manually generated mesh, by increasing the number of analyses points it is possible to observe the variation of the electric field as a function of position in much greater detail.

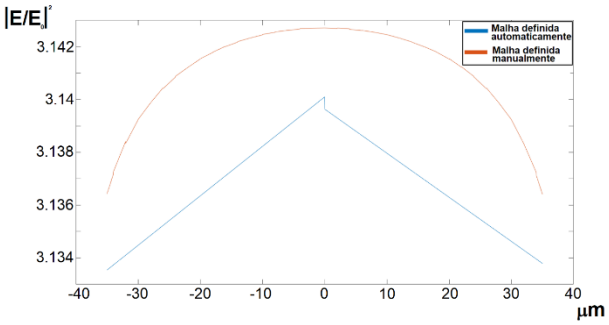


*Figure 18 - Comparison between the electric field received for an automatic mesh and for a manual mesh*

*D. Real Model Study*

After defining the mesh as manual, and having a good rigor in the results obtained, the simulations for the real model were started. This model consists of adding the layers of the skin to the platinum metallic elements model, so we are left with a sequence of 4 sections. The first section was the structure already analysed that is constituted by the nanoantenna, to the right of this was added the second section that represents the epidermis layer, to the right of the epidermis was added a third section that represents the dermis layer, lastly to the right of this was added a section that represents the hypodermis layer, the scheme of this model is represented in figure 37.

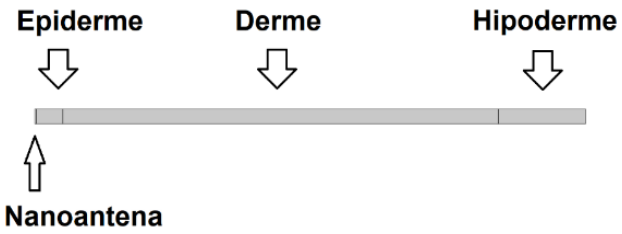


To perform this simulation 4 type scenarios were created, two of these scenarios correspond to a light-skinned Caucasian person and the other two correspond to a dark-skinned African person.

| ***light-skinned Caucasian (systole)*** | *epiderme* | *derme* | *hipoderme* |
|---|---|---|---|
| *Condutividade (S/m)* | 0.95 | 0.2 | 0.7 |
| *Índice de refração (Real)* | 1.40 | 1.39 | 1.40 |
| *Índice de refração (Imaginário)* | $5*10^{-5}$ | $5*10^{-6}$ | $2.5*10^{-4}$ |
| *Espessura da camada (µm)* | 140 | 4700 | 470 |
| ***light-skinned Caucasian (diastole)*** | | | |
| *Condutividade (S/m)* | 0.95 | 0.2 | 0.7 |
| *Índice de refração (Real)* | 1.45 | 1.39 | 1.40 |
| *Índice de refração (Imaginário)* | $5*10^{-5}$ | $5*10^{-6}$ | $2.5*10^{-5}$ |
| *Espessura da camada (µm)* | 140 | 4700 | 470 |
| ***dark-skinned African (systole)*** | | | |
| *Condutividade (S/m)* | 0.95 | 0.2 | 0.7 |
| *Índice de refração (Real)* | 1.45 | 1.39 | 1.45 |
| *Índice de refração (Imaginário)* | $5*10^{-5}$ | $5*10^{-6}$ | $2.5*10^{-4}$ |
| *Espessura da camada (µm)* | 140 | 4700 | 470 |
| ***Dark-skinned African(diastole)*** | | | |
| *Condutividade (S/m)* | 0.95 | 0.2 | 0.7 |
| *Índice de refração (Real)* | 1.45 | 1.39 | 1.45 |
| *Índice de refração (Imaginário)* | $5*10^{-5}$ | $5*10^{-6}$ | $2.5*10^{-5}$ |
| *Espessura da camada (µm)* | 140 | 4700 | 470 |

In order to analyze the magnetic field variation, new cutlines were added to the model. The cutlines are located at the ends of the borders between the different sections, the sensor cutline is located between the sensor and the epidermis, the epidermis cutline is located between the epidermis and the dermis, the dermis cutline is located between the dermis and the hypodermis, finally the hypodermis cutline is located at the right end of our scheme. The small variations in the model data were purposely introduced to demonstrate that the sensitivity of an oximeter must be high to detect the smallest variations. Below

are the graphs with the data obtained from the simulation for the Caucasian individual and the African individual.

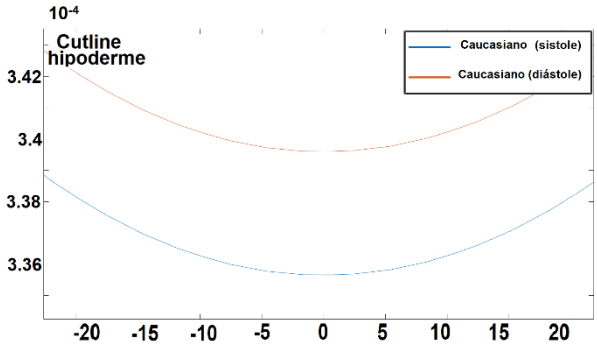


*Figura 19 - resultados da simulação cutline hipoderme para um individuo caucasiano*

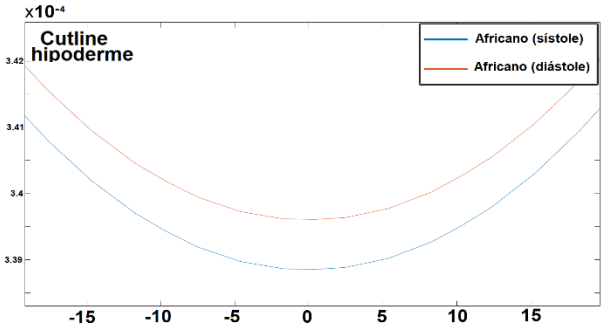


*Figura 20 - Resultados da simulação cutline hipoderme para um individuo africano*

During the systole phase there is an increase in the amount of blood in the capillary vessels, which according to Figure 6, for the length of 950 nm, will cause a greater attenuation due to the high amount of oxygen-rich blood that travels through the veins. In this way we can state that for both the Caucasian and the African individual it is possible to observe in the previous figures that the electric field for the case of systole is always lower compared to diastole, which is in accordance with what was expected. From this model we can conclude that the model can be applied to calculate the electric field when it travels through the layers of the skin

## 5. CONCLUSION

In this work we started with an introduction of the fundamental chapter that are necessary to understand the theme of this master thesis. First were presented concepts related to the application of nanoantenna and biosensors, as well as the topic of biometric parameters of the human body. After that it was presented de fundamental of pulse oximetry, and how it works. The limitations of the oximetry were also presented as well as the advantages and disadvantages of its use compared to other similar technologies. In the results chapter, the COMSOL simulation tested the behaviour of the nanoantenas and which combination of arrangement were the best. After the determination of the optimal characteristics of the nanoantenna, a real model was tested to understand how the electric field would propagate through the skin layers. At the end we can conclude that the model describes de behaviour of the electric field as we expected to be.

## REFERENCES


[1] I. Blumenthal, “THE DEVELOPMENT OF THE CLINICAL THERMOMETER,” 1998.

[2] O. S. Fathabadi, T. J. Gale, J. C. Olivier, and P. A. Dargaville, “Automated control of inspired oxygen for preterm infants: What we have and what we need,” *Biomedical Signal Processing and Control*, vol. 28. Elsevier Ltd, pp. 9–18, Jul. 01, 2016. doi: 10.1016/j.bspc.2016.03.002.

[3] G. C. Gutiérrez-Tobal, M. L. Alonso-Álvarez, D. Álvarez, F. del Campo, J. Terán-Santos, and R. Hornero, “Diagnosis of pediatric obstructive sleep apnea: Preliminary findings using automatic analysis of airflow and oximetry recordings obtained at patients’ home,” *Biomedical Signal Processing and Control*, vol. 18, pp. 401–407, 2015, doi: 10.1016/j.bspc.2015.02.014.

[4] K. Li, S. Warren, and B. Natarajan, “Onboard tagging for real-time quality assessment of photoplethysmograms acquired by a wireless reflectance pulse oximeter,” *IEEE Transactions on Biomedical Circuits and Systems*, vol. 6, no. 1, pp. 54–63, Feb. 2012, doi: 10.1109/TBCAS.2011.2157822.

[5] J. Abd Sukor, M. S. Mohktar, S. J. Redmond, and N. H. Lovell, “Signal quality measures on pulse oximetry and blood pressure signals acquired from self-measurement in a home environment,” *IEEE Journal of Biomedical and Health Informatics*, vol. 19, no. 1, pp. 102–108, Jan. 2015, doi: 10.1109/JBHI.2014.2361654.

[6] T. Tamura, Y. Maeda, M. Sekine, and M. Yoshida, “Wearable photoplethysmographic sensors—past and present,” *Electronics* , vol. 3, no. 2. MDPI AG, pp. 282–302, Apr. 23, 2014. doi: 10.3390/electronics3020282.

[7] D. Li, H. Zhao, and S. Dou, “A new signal decomposition to estimate breathing rate and heart rate from photoplethysmography signal,” *Biomedical Signal Processing and Control*, vol. 19, pp. 89–95, May 2015, doi: 10.1016/j.bspc.2015.03.008.

[8] R. Jaafar and M. A. A. Rozali, “Estimation of breathing rate and heart rate from photoplethysmogram,” in *Proceedings of the 2017 6th International Conference on Electrical Engineering and Informatics: Sustainable Society Through Digital Innovation, ICEEI 2017*, Mar. 2018, vol. 2017-November, pp. 1–4. doi: 10.1109/ICEEI.2017.8312414.

[9] F. de Engenharia, D. Fonseca Cruz, D. Carlos Manuel Pereira Cabrita Coorientador, and D. Eduardo Manuel Godinho Rodrigues, “UNIVERSIDADE DA BEIRA INTERIOR Sensor de Fotopletismografia por Reflexão sem Fios: Projeto e Desenvolvimento de Hardware.”

[10] A. E. Krasnok *et al.*, “Optical nanoantennas,” *Uspekhi Fizicheskih Nauk*, vol. 183, no. 6, pp. 561–589, 2013, doi: 10.3367/ufnr.0183.201306a.0561.

[11] “4. Sensores/Transdutores 4.1. Conceitos Gerais.”

[12] J. Lee and K. H. Chon, “Time-varying autoregressive model-based multiple modes particle filtering algorithm for respiratory rate extraction from pulse oximeter,” *IEEE Transactions on Biomedical Engineering*, vol. 58, no. 3 PART 2, pp. 790–794, Mar. 2011, doi: 10.1109/TBME.2010.2085437.

[13] R. G. Haahr *et al.*, “An electronic patch for wearable health monitoring by reflectance pulse oximetry,” *IEEE Transactions on Biomedical Circuits and Systems*, vol. 6, no. 1, pp. 45–53, Feb. 2012, doi: 10.1109/TBCAS.2011.2164247.

[14] J. G. Webster, *Design of pulse oximeters*. Institute of Physics Pub, 1997.

[15] G. Pang and C. Ma, “A Neo-Reflective Wrist Pulse Oximeter,” *IEEE Access*, vol. 2, pp. 1562–1567, 2014, doi: 10.1109/ACCESS.2014.2382179.

[16] K. M. Warren, J. R. Harvey, K. H. Chon, and Y. Mendelson, “Improving pulse rate measurements during random motion using a wearable multichannel reflectance photoplethysmograph,” *Sensors (Switzerland)*, vol. 16, no. 3, Mar. 2016, doi: 10.3390/s16030342.

[17] C. Y. Huang, M. C. Chan, C. Y. Chen, and B. S. Lin, “Novel wearable and wireless ring-type pulse oximeter with multi-detectors,” *Sensors (Switzerland)*, vol. 14, no. 9, pp. 17586–17599, 2014, doi: 10.3390/s140917586.

[18] P. D. Mannheimer, J. R. Casciani, M. E. Fein, and S. L. Nierlich, “Wavelength Selection for Low-Saturation Pulse Oximetry,” 1997.

[19] E. Mohajerani, “Mechanisms of Laser-Tissue Interaction: I. Optical Properties of Tissue,” 2011. [Online]. Available: https://www.researchgate.net/publication/267219129

[20] I. v. Meglinski and S. J. Matcher, “Quantitative assessment of skin layers absorption and skin reflectance spectra simulation in the visible and near-infrared spectral regions,” *Physiological Measurement*, vol. 23, no. 4, pp. 741–753, Nov. 2002, doi: 10.1088/0967-3334/23/4/312.

[21] “BIOMEDICAL OPTICS.”

[22] Steven L. Jacques, “https://omlc.org/news/jan98/skinoptics.html,” *Oregon Medical Laser Center News*, Jan. 1998.

[23] D. J. Segelstein, “https://omlc.org/spectra/water/data/segelstein81.txt,” *The complex refractive index of water, University of Missouri-Kansas City*, 1981.

[24] Steven Jackes, “https://omlc.org/spectra/melanin/.”

[25] Steven Jacques, “https://omlc.org/spectra/melanin/extcoeff.html.”